

Augmented doppler filter bank based approach for enhanced targets detection

Abstract. Radar Target Detection (RTD) is considered to be one of the most essential parts of modern radar systems. In typical radars, detecting targets in noise is difficult. Conventional radar signal processing approaches such as Constant False Alarm Rate (CFAR) are adopted in an attempt to improve the Signal-to-Noise Ratio (SNR). However, due to the severity of the harsh and complex environments in the radar measurements, the target detection problem becomes extremely challenging when employing such traditional approaches. Therefore, developing a reliable and robust RTD technique is essential. In this paper, an augmented Doppler Filter Bank (DFB) based approach has been proposed to handle the associated radar drawbacks in such a complicated scenario, by incorporating the computer vision algorithms in order to separate the moving targets from the noisy background through a real radar dataset. A Frequency Modulated Continuous Wave (FMCW) radar has been mounted on an Unmanned Aerial Vehicle (UAV) for ground targets detection purposes. A real flight has been conducted in a challenging environment to assess the performance of the proposed system. The experimental results demonstrate the ability of the proposed system to enhance the estimated forward velocity to 82.8% over the conventional DFB with the CFAR detector.

Streszczenie. radarowe wykrywanie celu (RTD) jest uważany za jedną z najważniejszych części nowoczesnych systemów radarowych. W typowych radarach wykrywanie celów w hałasie jest utrudnione. Konwencjonalne podejścia do przetwarzania sygnału radarowego, takie jak stała częstotliwość fałszywych alarmów (CFAR), są stosowane w celu poprawy stosunku sygnału do szumu (SNR). Jednak ze względu na surowość trudnych i złożonych środowisk w pomiarach radarowych, problem wykrywania celu staje się niezwykle trudny przy stosowaniu takich tradycyjnych podejść. Dlatego niezbędne jest opracowanie niezawodnej i solidnej techniki BRT. W tym artykule zaproponowano podejście oparte na rozszerzonym banku filtrów dopplerowskich (DFB), aby poradzić sobie z powiązаныmi wadami radaru w tak skomplikowanym scenariuszu, poprzez włączenie algorytmów widzenia komputerowego w celu oddzielenia ruchomych celów od hałaśliwego tła za pomocą prawdziwego radaru zestaw danych. Radar fali ciągłej z modulacją częstotliwości (FMCW) został zamontowany na bezałogowym statku powietrznym (UAV) w celu wykrywania celów naziemnych. Aby ocenić działanie proponowanego systemu, przeprowadzono prawdziwy lot w trudnym środowisku. Wyniki eksperymentów pokazują zdolność proponowanego systemu do zwiększenia szacowanej prędkości do przodu do 82,8% w porównaniu z konwencjonalnym DFB z detektorem CFAR. (Podejście oparte na rozszerzonym banku filtrów dopplerowskich do ulepszonego wykrywania celów)

Keywords: constant false alarm rate, doppler filter bank, moving target detector, radar signal processing.

Słowa kluczowe: stała częstość fałszywych alarmów, bank filtrów dopplerowskich, wykrywacz ruchomych celów, przetwarzanie sygnału radarowego.

Introduction

Over the last decade, radars have played a vital role in numerous technologies for detection and tracking purposes, these systems are important due to their ability to operate with reasonable precision under diverse weather conditions. Furthermore, these systems have the ability to provide valuable information in terms of the range, azimuth, height, and speed of the targets.

The development of modern radars has been established during the last decade to adopt the increased requirements for superior radar performance in all aspects of civil applications such as automotive radar, air traffic control, aircraft navigation, remote sensing and the environment, ship navigation and safety, law enforcement, and in many other fields such as commercial, industrial, and medical applications. On the other hand, radar systems have been conducted in military applications such as land-based air defense radar, missile control radar, airborne fire control radar, airborne surveillance radar, coastal and naval surveillance, and navigation radar[1].

Although these radars demonstrated their ability to operate in diverse and severe environmental conditions, their measurement accuracy is still affected by many factors, such as harsh environments, the maneuverability of the moving targets under strong clutter and interference conditions, and the targets that have a low signal-to-noise ratio. Hence, there is a significant necessity to develop robust and efficient approaches for detecting and classifying moving targets [2].

RTD and information extraction are considered to be one of the most widely utilized techniques to determine the presence of the desired target's echo signals among the noisy measurements since the reflected echo signals are

often immersed in complex backgrounds such as noise, clutter, and jamming.

One of the essential components of RTD is digital signal processing, which is employed to discriminate between stationary and moving targets, such as a Moving Target Detector (MTD) [3].

DFB is considered to be the core element of the MTD, which consists of collection filters that are conducted for target detection purposes inside the MTD. Radar receive signals from many sources. These signals are then sorted in the DFB depending on their Doppler frequency. DFBs were realized by employing the Fast Fourier Transform (FFT) algorithm. The filters in the bank are designed in such a way that it passes narrow band frequencies depending on the number of samples for the received signal [4].

CFAR follows the MTD, and it is able to detect real targets by comparing the sample value with a threshold at each Pulse Repetition Interval (PRI). According to some a priori knowledge about clutter situations, the threshold is estimated. It is determined that the accuracy of the CFAR depends on the statistical properties of the signal and the probability of detection. The effective accuracy of radar is determined by its probability of detection (P_d) and probability of false alarms (P_{FA}) [5].

Machine Learning (ML) has been investigated by many researchers toward obtaining an intelligent signal processing technique that has the ability to perform the target detection process by using different strategies. The proposed algorithms aim to merge the radar measurements and parameters with the appropriate ML algorithms, such as empowerment techniques, Decision Tree (DT), Random Forest (RF), and Support Vector Machine (SVM). Automatic

feature learning is also included such as Deep Learning (DL) and Deep Belief Networks (DBN), Feed Forward Neural Networks (FNN), Deep Reinforcement Learning (DRL), Auto Encoder (AE), Long-Short Term Memory (LSTM), Recurrent Neural Networks (RNN), Convolutional Neural Networks (CNN), and Generative Adversarial Networks (GAN) [6,7].

Although most of the employed ML and DL in modern radar have a great benefit over the traditional radar signal processing techniques toward improving the probability of detection and mitigating the false alarm rate, their accuracies are still affected by the amount of training data. Furthermore, the complexity of such trained models increases the consumed time for detecting the targets [8].

This paper presents an alternative and robust system which has the capability of handling the associated drawbacks with both the conventional and the combined RTD with the various ML algorithms. The main contributions of the proposed system are: First, it has the ability to increase the probability of detection and decrease the probability of false alarm for the desired targets than the CFAR detector by employing computer vision algorithms such as Otsu's multi-level thresholding algorithm to segment the moving targets from the noisy background as well as using Random Sample Consensus (RANSAC) algorithm for outliers' rejection purposes. Second, a performance evaluation has been conducted on the proposed system through a real dataset that has been gathered during two flights in different complicated environments to demonstrate its feasibility of detecting the targets in such harsh scenarios. Third, the proposed approach reduces the consumed time for the target detection process more than the ML and DL approach since it doesn't rely on a complicated trained model, which makes it more suitable for real-time applications. Finally, Experimental results show that the proposed system outperforms MTD radar processors with DFB and CFAR for target detection. The detected targets from both systems are then exploited to estimate the vehicle forward velocity and compare it with the ground truth vehicle velocity obtained from the GPS/INS integration. The results demonstrate the capability of the proposed augmented DFB system to reduce the RMS forward velocity errors to 82.8% more than the conventional DFB with the CFAR detector.

The organization of this paper is as follows: Section 2 discusses related work on RTD including traditional DFB and CFAR detectors. The system overview of the proposed algorithm is presented in Section 3. The experimental results are presented and discussed in section 4. Finally, the conclusions are given in Section 5.

Related Work on Radar Target Detection

Echo signals from the radar are often affected by noise, clutter, and jamming; during radar signal processing, the reflected signals from the radar are processed by various systems such as matched filtering, DFB, zero velocity filter, CFAR detection, etc. In order to achieve a narrow pulse width and high-range resolution, the radar signal is sampled at a certain rate, then compressed by a matched filter. Range-Doppler spectrum maps are obtained by applying Doppler processing to multiple pulses at each range unit. The CFAR detector determines which Range-Doppler signal has larger energy than the detection threshold by analyzing the reflected signal amplitude stored in separate cells. Low Doppler targets and clutters are isolated by zero velocity filters, and then a clutter map and threshold detector are applied to the output. After this, the velocity and position of the target can be determined [1].

This traditional approach uses statistical hypothesis

testing to establish an adaptive detection threshold, which varies depending on the levels of clutter and noise energy. As a result, if a threshold is set too low, more targets will be detected, but false alarms will increase. On the other hand, if the threshold is set too high, a low number of false alarms is expected, but the number of targets detected will decrease [2].

Recently, various ML-based approaches have been explored by researchers for target detection purposes. Hu and Qi present a method for developing an adaptive detector [10]. Their method utilizes a Neural Network-based approach to determine whether the background contains multiple targets, clutter transitions, or homogeneous noise, and then decide the appropriate CFAR for the estimated environment. Khalid et al. Research on radar Range-Doppler for automatic target recognition using Convolutional Long Short-Term Memory (CLSTM) [11]. Akhtar and Olsen have developed a method for training an ANN using a CA-CFAR and fixing the errors of the CA-CFAR, resulting in a lower (P_{FA}) [12]. Due to the intrinsic ability of neural networks to learn features from input data, Thornton uses neural networks to solve the radar clutter classification problem [13]. Numerous research has been developed over time to exploit convolutional neural networks for the sake of radar target identification in complex, nonstationary, and cluttered scenes. A signal detector has been developed based on a joint time-frequency analysis of radar imagery for target detection [14,15]. Afterward, an alternative approach was developed for target detection by sending the Range-Doppler spectrum to CNN instead of a time-frequency analysis of radar imagery [16]. An ML based on DT was proposed by Deng et al. for target detection [17]. A CNN detector for single targets in homogeneous interference was developed by Yavuz et al [18]. Akhtar et al. presented an ANN-CFAR detector that can detect fluctuating targets in noisy backgrounds. Clutter detection is more common but more challenging than detecting targets within noise backgrounds [19]. Although most of the previously employed ML and DL in modern radar has a great benefit over the traditional radar signal processing techniques toward improving the probability of detection and mitigating the false alarm rate, their accuracies are still affected by the amount of training data. Furthermore, the complexity of such trained models increases the consumed time for detecting the targets.

System Overview

In this section, the hardware setup has been introduced for the proposed augmented DFB system which attempts to tackle the associated challenges with the conventional signal processing techniques and to improve the RTD by segmenting the noisy background from the desired echo signals. Fig. 1 demonstrates the proposed system's block diagram.

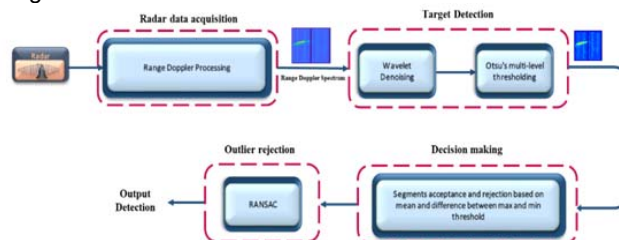


Fig.1. Radar target detection system block diagram

Hardware Setup

The operational frequency of the utilized FMCW radar is 24 GHz. The radar has a resolution of 0.1 degrees, a +/- 10-degree elevation-plane accuracy, and a +/- 15-degree

azimuth-plane accuracy. It is composed of three receivers microstrip patch antennas and one transmitter. With a resolution of 1 meter, the radar can detect objects up to 100 meters away from people and 300 meters away from vehicles.

The Quadcopter is mainly controlled by Pixhawk-2 autopilot which is equipped with multiple sensors such as MS5611 barometer, U-Blox GPS, and InvenSense MPU-6000 MEMS IMU. During the flights, the payload (420g) for the experiments comprises the radar system at the UAV belly connected through ethernet to a BULLET-M, 2.4 GHz 28dBm transmitter with Omni direction antenna (BM2HP by Ubiquity) with the ability to transmit 100+ Mbps. On the other side, a Nano Station-M is connected to the ground station to collect the data from the radar as shown in Fig. 2.

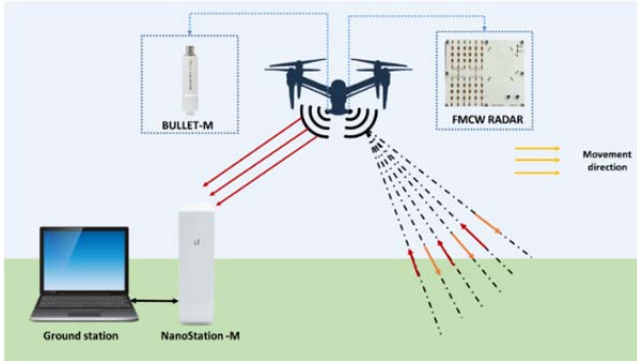


Fig.2. Hardware setup configuration

Radar Data Acquisition

FMCW radar has been mounted on a UAV to detect moving targets. A frequency-modulated sawtooth chirp is continuously emitted by the attached micro-radar throughout the flight $f_{RF\ TX}$ across the ground objects can be expressed as:

$$(1) \quad f_{RF\ TX} = f_c + \alpha t \quad , 0 \leq t < T$$

$$(2) \quad \alpha = \frac{B}{T}$$

Where f_c is the carrier frequency, α is the frequency sweep rate, B is the transmitted chirp signal bandwidth and T is the frequency sweep time.

Signals are transmitted towards the target and the reflected signal is obtained at the receiver with a small frequency shift Δf and a propagation time delay Δt between the two-radiated frequency. These frequency and time delays occur as a result of the range propagation influence. The propagation delay time between the received and the transmitted signals is given by:

$$(3) \quad \Delta t = 2 \frac{R}{c}$$

Where c is the speed of light, and R is the range between the radar antenna and each scatterer inside the beam width of the radar. The frequency of the received signal is shifted by the time delay Δt as:

$$(4) \quad f_{RF\ RX} = f_c + \alpha * (t - \Delta t) \quad , \Delta t \leq t < T + \Delta t$$

The received signal is then mixed with the originally transmitted signal and passed through a low pass filter to obtain the video signal $x(t)$ that has a low differential frequency or Beat frequency f_b as follows:

$$(5) \quad f_b = \alpha * \Delta t$$

By substituting from Eqn. (2,3) in Eqn. (5), f_b can be rewritten as:

$$(6) \quad f_b = \frac{B}{T} * 2 \frac{R}{c}$$

The Doppler frequency $f_{doppler}$ is then extracted from the phase changes of this signal. This allows for determining the velocity of the target. The utilized radar has a 12.150 khz repetition rate for the transmitted chirps. In each chirp, 256 sampling points were taken with a sample rate of 264 ns.

A bank of Doppler filters is the core of the MTD signal processor which reduces clutter and noise, This Doppler filter bank is realized for MTD by the FFT algorithm.

A baseband signal is generated by digitizing the received radar signal after it has been digitized using an A/D converter. In order to make the target decision, a series of algorithms for the proposed system after Range-Doppler processing is based on FFT. After sampling the received signal, the first step is to perform an FFT so that there is a correspondence between each sample and a "bin" to determine the range information over the "fast time". The procedure is repeated for every chirp that forms a frame. As soon as all the chirps in a frame are acquired and processed, doppler-FFT is performed to determine the target's velocity. Every N chirp, this evaluation is performed once per frame. Due to this, it is also referred to as "slow time." Finally, the third dimension of the radar cube contains information about the target's spatial position, which is derived from the combined spatial information along all channels. After applying the FFT for the sampled signals, a mean Range-Doppler Map (RDM) is generated that has 256x256 pixels with a 32-Bit amplitude value for each pixel. Fig. 3 demonstrates the RDM image where the horizontal axis provides the speed measurements while the vertical axis presents the range measurements. Each pixel has a 32-Bit value to represent the strength of the received signals from various earth scatters. This constructed image is then exploited for detecting targets [20, 21].

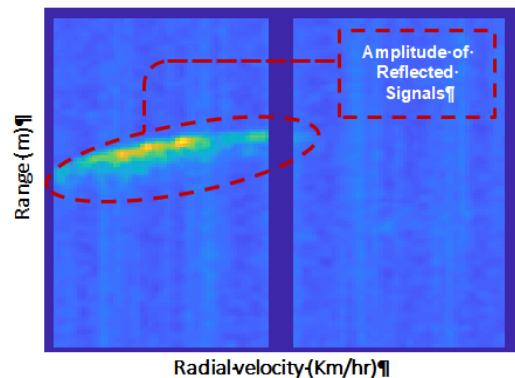


Fig.3. Reflected ground signals in the RDM image

Target Detection Wavelet denoising

The acquired RDM contains random noises which are affecting the accuracy of the detected targets and the estimated vehicle forward velocity from the RDM as well. There are different denoising schemes to remove such random noise while preserving the remaining original image information such as the edges, contrast, brightness, and background of the image. Wavelet transform is one of the effective algorithms utilized for denoising purposes. The wavelet technique for image denoising is based on the threshold function and calculated by:

$$(7) \quad TH = \sqrt{2m * \log(p)}$$

Where m is the mean of the image, and p is the total number of pixels of the image. This threshold function is calculated at the different scale level [22].

Otsu's Multi-Level Thresholding

The denoised RDM image is then segmented into multiple layers based on Otsu's multi-level thresholding algorithm. As a general rule, automatic thresholding involves selecting an optimal gray-level threshold value based on the gray-level distribution of objects of interest in an image to separate them from the background [23].

By using gray values as the basis for the image and selecting a convenient threshold for separating the target from the background, in order to calculate the maximum variance between the background and foreground of an image, the maximum inter-class variance threshold image segmentation method is used.

In general, the greater the variance in this method, the greater the difference between the two parts [24]. The fundamental idea behind the threshold segmentation algorithm based on the OTSU is described in the following: Considering an image with L gray levels $[0, 1, 2, \dots, L-1]$, n_i is the number of pixels at level i , and the total number of pixels is given by $N = n_1 + n_2 + \dots + n_L$. The probability of the gray level i is given by:

$$(8) \quad p_i = \frac{n_i}{N}, \quad p_i \geq 0$$

pixels of An image are divided into two classes C_0 and C_1 according to the bi-level thresholding method at gray level threshold t such that $C_0 = \{0, 1, 2, \dots, t\}$ and $C_1 = \{t+1, t+2, t+3, \dots, L-1\}$. For the two classes, the gray level probability distributions are as follows:

$$(9) \quad \omega_0 = \sum_{i=0}^t p_i$$

$$(10) \quad \omega_1 = \sum_{i=t+1}^{L-1} p_i$$

As a result, the means of the two classes can be calculated as follows:

$$(11) \quad \mu_0 = \frac{\sum_{i=0}^t i p_i}{\omega_0}$$

$$(12) \quad \mu_1 = \frac{\sum_{i=t+1}^{L-1} i p_i}{\omega_1}$$

The total mean μ_T of the gray levels is calculated as follows:

$$(13) \quad \mu_T = \omega_0 \mu_0 + \omega_1 \mu_1$$

The class variances are calculated as follows:

$$(14) \quad \sigma_0^2 = \frac{\sum_{i=0}^t (i - \mu_0)^2 p_i}{\omega_0}$$

$$(15) \quad \sigma_1^2 = \frac{\sum_{i=t+1}^{L-1} (i - \mu_1)^2 p_i}{\omega_1}$$

The within -class variance is calculated as:

$$(16) \quad \sigma_W^2 = \sum_{K=1}^M \omega_K \sigma_K^2$$

The between-class variance is calculated as:

$$(17) \quad \sigma_B^2 = \omega_0 (\mu_0 - \mu_T)^2 + \omega_1 (\mu_1 - \mu_T)^2$$

The total variance of the gray levels is calculated as follows:

$$(18) \quad \sigma_T^2 = \sigma_W^2 + \sigma_B^2$$

According to the Otsu method, the optimum threshold t is selected by maximizing the between-class variance, which is the same as minimizing the variance within-class variance, since the total variance for different partitions is constant; the optimal threshold t is calculated as follows:

$$(19) \quad t = \text{Arg}\{\max_{0 \leq i \leq L-1} \{\sigma_B^2(t)\}\}$$

$$= \text{Arg}\{\max_{0 \leq i \leq L-1} \{\sigma_W^2(t)\}\}$$

In addition to the Otsu method, a multilevel thresholding method can be implemented. Assuming that there are $M-1$ thresholds $[t_1, t_2, t_3, \dots, t_{M-1}]$ that divide the Image pixels to M classes $[c_1, c_2, c_3, \dots, c_M]$ the result will be as follows:

$$(20) \quad [t_1, t_2, t_3, \dots, t_{M-1}] = \text{Arg}\left\{\max_{0 \leq i \leq L-1} \{\sigma_B^2(t_1, t_2, t_3, \dots, t_{M-1})\}\right\}$$

$$= \text{Arg}\left\{\max_{0 \leq i \leq L-1} \{\sigma_W^2(t_1, t_2, t_3, \dots, t_{M-1})\}\right\}$$

In the Otsu method, the optimum threshold t is determined by maximizing the between-class variance σ_B^2 , which is the same as minimizing the within-class variance σ_W^2 , since the total variance $\sigma_T^2 = \sigma_W^2 + \sigma_B^2$ remains constant for given image. After performing the multiple thresholding segmenting process on the RDM image, a heat map (colored spectrum) image is created to discriminate the boundaries of each segment from the others segments as shown in Fig. 4.

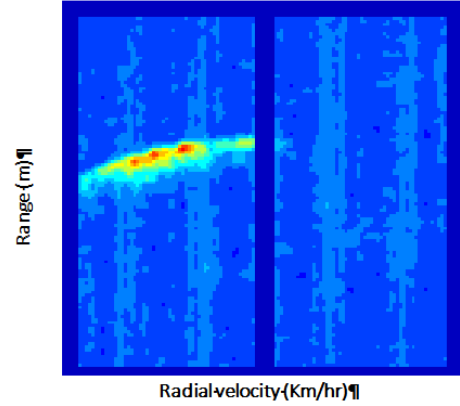


Fig.4. segmented image by proposed Otsu multilevel thresholding

The decomposed segments of the RDM image have been demonstrated in Fig. 5 after applying the Otsu multilevel thresholding algorithm.

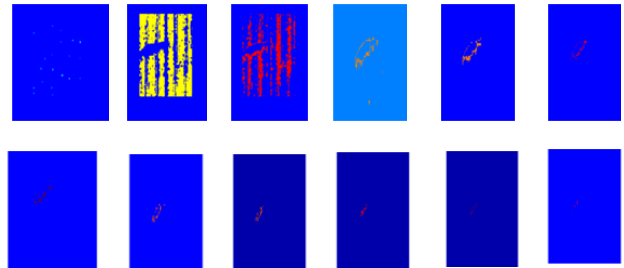


Fig.5. Otsu multilevel thresholding algorithm Image decomposition

Decision Making

In order to separate the foreground targets from the noisy background, two thresholds have been conducted based on the mean of the target velocity, and the velocity spread (difference between max and min velocity values on the RDM image). The proposed thresholds demonstrate their ability to successfully reject noisy background segments from the image foreground. The main concept behind the employed thresholds is that they exploit the boundary limitations of the measured speed by the radar for the detected targets. Since the utilized radar is capable of measuring the detected target's velocity up to 5 m/sec and the sign representing the direction of the target motion with respect to the radar, the target velocity will not exceed this limit. Therefore, any scatters that have a velocity exceeding this limit (0 to 5 m/sec) will be treated as a noisy background. In addition, it has been noticed that the noisy background is spread over a large area of the RDM image and covers a large range of velocities values approximately from -5 up to +5 m/sec. Based on this fact, the mean of the velocity's values for the background will be a very small value (almost near zero) and the spread of the velocity's values will be greater than the maximum allowed value, which is 5 m/sec.

Fig. 6 illustrates a histogram for the velocities distribution over each segment of the RDM image. These histograms are utilized to estimate the mean and spreading thresholds level for each segment to decide whether to accept or reject this segment.

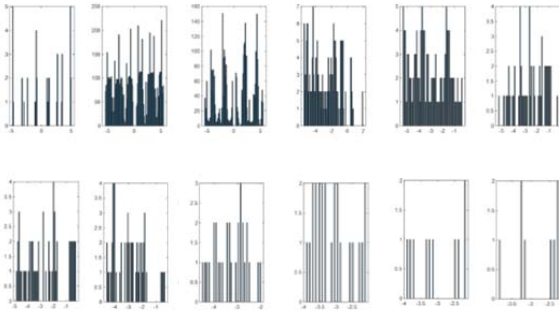


Fig.6. histogram for the whole RDM segmented image

These histograms are utilized to estimate the mean and spreading thresholds level for each segment to decide whether to accept or reject. Fig. 7 shows the unwanted removed background after applying the decision-making process.



Fig.7. unwanted removed background

Outlier Rejection by RANSAC Algorithm

The RANSAC algorithm is utilized for outliers (incorrect matches) rejection in each segment. The RANSAC is applied to resample each segment in the RDM iteratively. With this recursive approach, a minimum number of observations (data points) is used in order to estimate the parameters of the underlying model, and candidates are generated. To generate an initial solution, RANSAC uses the smallest possible set and then prunes outliers [25]. The basic idea of the RANSAC algorithm is described as follows:

- 1) determine the model parameters by choosing at random the minimum number of points. Calculate model parameters from the samples.
- 2) calculate the number of points that fit within a predefined tolerance from the set of all points.
- 3) it is recommended to re-estimate the model parameters if the ratio of the total number of points to the number of inliers exceeds the threshold of a predefined.

The same procedure is repeated approximately a fixed number of times, resulting in either a model that is denied because there are not enough points in the refined model with an appropriate consensus set size. In such a case, the refined model is saved if its consensus set is greater than the previous model that was saved.

An appropriate number of iterations, N , is chosen high enough in order to ensure that there is no outlier in the probability p that at least one of the sets of random samples. Consider u to be the probability that any selected data point is an inlier and the probability of observing an outlier is $v = 1 - u$. The minimum number of points m for N iterations are required, where

$$(21) \quad 1 - p = (1 - u^m)^N$$

Thus, by manipulating some parameters,

$$(22) \quad N = \frac{\log(1-p)}{\log(1-(1-u)^m)}$$

Fig. 8 illustrates the resulted segments after applying the RANSAC algorithm for outlier's rejection and Fig. 9 illustrates the gathered segments after removing the noisy background and rejecting the outlier's.

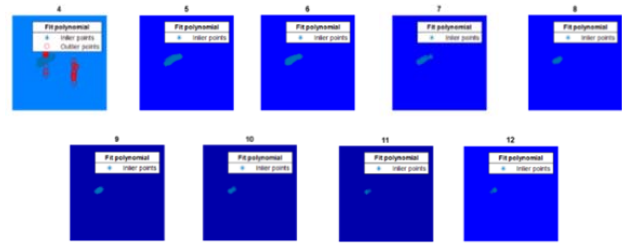


Fig.8. resulted segments after applying the RANSAC algorithm

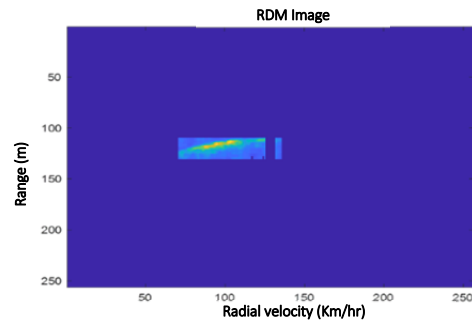


Fig.9. gathered segments after removing the noisy background and rejecting the outlier's

Experimental Results

A real flight with Solo Quadcopter has been performed over a farm which includes a variety of objects at various altitudes such as houses, hangars, trees, and cars in order to assess the proposed method's performance for augmented DFB versus the conventional DFB with the CFAR detector. The utilized UAV has been equipped with Pixhawk-2 autopilot that contains InvenSense MPU-6000 MEMS Inertial Measurements Unit (IMU), U-Blox GPS, and MS5611 barometer. These sensors are utilized for positioning and localization purposes. The employed radar has been attached to the belly of the UAV and tilted toward the ground by 60 degrees to detect ground scatters. The flight trajectory involved 18 waypoints of a total flight duration of 393secs, with a maximum speed of 5m/s according to Fig. 10.

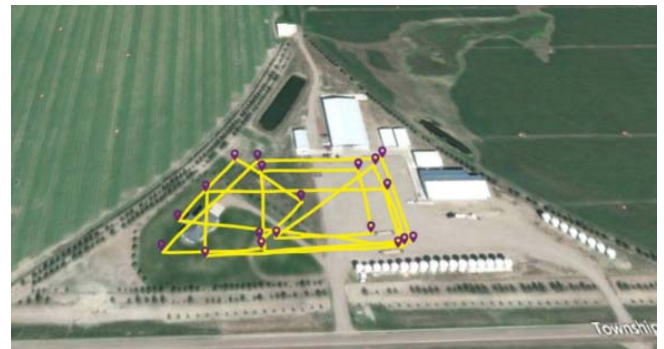


Fig.10. UAV flight trajectory

CFAR is widely deployed for radar target detection, which is utilized to separate out specific information from

the background of the received signals. CFAR is designed to detect targets by estimating the threshold power level adaptively and identifying them when the returned echo signal exceeds it, in this method of detection, the power of the Cell Under Test (CUT) compared with the power of its neighbours.

Although CFAR is an effective detection method for a variety of applications, such as airborne radars and ground radar stations, it does not fit the proposed system since ground scatters have similar power levels to RDMs, making it inconvenient for the proposed system. Fig. 11 shows the CFAR-detected targets in the RDM image where a part of the arc from the ground objects has been detected, though the rest has been missed.

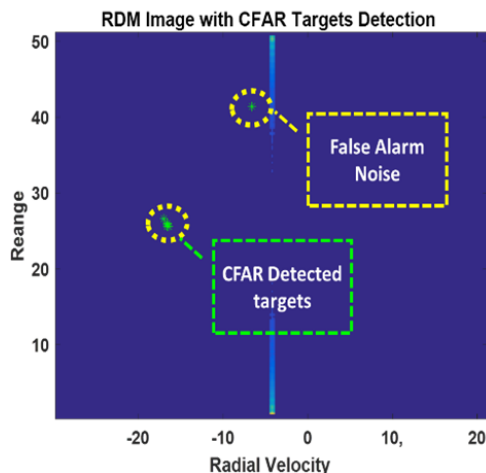


Fig.11. RDM image with CFAR target detection

In addition, CFAR detected an apparent false target (noise) with a prominent power level when compared with its background. The first challenge occurs when estimating CUT power from patched areas with real ground scatter while inside a patched area of CUT with a surrounding background. As a result of the CUT's power level being the same as its neighborhood, the CFAR was unable to detect all targets in this case. The second problem occurs as a result of random noise with a relatively high-power level in comparison to its local neighborhood.

Contrary to the CFAR, an alternative system based on computer vision algorithms (Augmented DFB) has been proposed to handle these limitations in such complicated and noisy environments. Since there is no information about the exact ground truth pixel size of the detected targets, it is impossible to estimate the probability of detection and false alarm. Therefore, another approach has been proposed for the sake of assessment and comparison between the proposed system and the conventional one. The estimated vehicle forward velocities from both the proposed system and the DFB with the CFAR detector are exploited to evaluate the performance of both systems with respect to the reference velocity which is obtained from the GPS/INS integration. The main reason for employing vehicle forward velocity is the direct correlation between the coordinates of the detected target and its corresponding velocity on the RDM image. Hence, the RMS errors on the estimated forward velocity will increase as long as incorrect scatters coordinates are treated as a detected target.

In Fig. 12, the estimated forward velocities from the augmented DFB, and the DFB with the CFAR detector are compared to the UAV reference forward velocity with RMS error values of 0.9, and 4.1 m/s respectively.

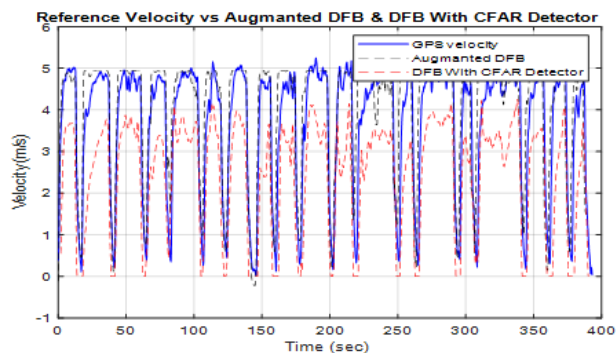


Fig.12. Comparison between forward ground truth velocity, which obtained from (GNSS/INS) integration, estimated velocity from the proposed augmented DFB, and the DFB with the CFAR detector.

Table.1 provides a comparison of the RMS error values for forwarding velocities from the augmented DFB, and the DFB with the CFAR detector is compared to the UAV reference forward velocity.

The results demonstrate the ability of the proposed system to reduce the average RMS velocity error to 17.2% relating to the reference velocity during the whole flight of the UAV.

Table 1.

Symbol	Symbol	RMS Error During [393 sec]
Forward Velocity Error	Augmented DFB	0.27
	DFB with the CFAR Detector	1.57

Conclusion

Target detection is an essential part of modern radar. This paper proposes an alternative system to replace an important processing part of conventional radar signal processing hypothesis testing. The main aim of the proposed system is to enhance the probability of detection by improving the accuracy of the estimated forward velocity for the detected targets in high-clutter environments over the conventional DFB with the CFAR detector. This goal has been achieved by employing a series of algorithms such as Wavelet denoising to reduce the random noise in RDM image, Otsu's multi-level thresholding algorithm to segment the moving targets from the noisy background, two thresholds based on the mean of the target velocity, and velocity spread to separate the foreground targets from the noisy background as well as using RANSAC algorithm for outlier's rejection purpose. Based on the gathered data during a real flight, a comparison between the performance of the proposed system versus the Conventional detectors based on Doppler filtering and CFAR detection has been performed. The experimental results demonstrate the proposed system's superiority in reducing the RMS forward velocity errors to 17.2% and enhancing the estimated forward velocity to 82.8% over the conventional DFB with the CFAR detector.

Authors: dr Mostafa M. Mostafa, Electronics and Electrical Communications Engineering Dept., Air Defence Collage, Alexandria, Egypt, Mahmoud Shaker, Electronics and Electrical Communications Engineering Dept., Air Defence Collage, Alexandria, Egypt, dr Shady Zahran, Department of Geomatics, University of Calgary, Calgary, Canada, prof. dr Mohamed EL-Said Nasr, Electronics and Electrical Communications Engineering Dept., Faculty of Engineering, Tanta University, Tanta 31527, Egypt, dr Azhar A. Hamdi, Department of Electronics and Communication, Zagazig University, Egypt. E-mail: mahmoudshaker037@gmail.com

REFERENCES

- [1] T. Long, Z. Liang and Q. Liu, "Advanced technology of high-resolution radar: Target detection, tracking, imaging, and recognition," *Science China. Inf. Sci.*, vol. 62 (4), no. 40301 pp. 1–26, 2019.
- [2] F. Gini, "Grand challenges in radar signal processing," *Frontiers Signal Process.*, vol. 1, pp. 1–6, 2021.
- [3] W. Sun, M. Sun, X. Zhang and M. Li, "Moving vehicle detection and tracking based on optical flow method and immune particle filter under complex transportation environments," *Complexity*, vol. 2020, no. 16, pp. 1–15, 2020.
- [4] Aubry, A. De Maio and M. M. Naghsh, "Optimizing Radar Waveform and Doppler Filter Bank via Generalized Fractional Programming," *IEEE Journal of selected topics in signal processing*, vol. 9, no. 8, pp. 1387–1399, 2015.
- [5] J. R. Machado-Fernández, N. Mojena-Hernández and J. d. I. C. Bacallao-Vidal, "Evaluation of cfar detectors performance," *Iteckne*, vol. 14, no. 2, pp. 170–178, 2017.
- [6] E. Mason, B. Yonel and B. Yazici, "Deep learning for radar," in *Proc. IEEE Radar Conf. (RadarConf)*, Seattle, WA, USA, pp. 1703–1708, 2017.
- [7] L. Wang, J. Tang and Q. Liao, "A study on radar target detection based on deep neural networks," *IEEE Sensors Letters*, vol. 3, no. 3, pp. 1–4, 2019.
- [8] P. Lang, X. Fu, M. Martorella, J. Dong, R. Qin et al., "A comprehensive survey of machine learning applied to radar signal processing," *arXiv:2009.13702*, 2020.
- [9] A. Jalil, H. Yousaf and M. Baig, "Analysis of CFAR techniques". In: *2016 13th International Bhurban Conference on Applied Sciences and Technology (IBCAST)*. IEEE, Islamabad, Pakistan, pp. 654–659, 2016.
- [10] Q. Qi and W. Hu, "One efficient target detection based on neural network under homogeneous and non-homogeneous background," *Inter-national Conference on Communication Technology Proceedings, ICCT, Chengdu, China*, vol. 2017, pp. 1503–1507, 2018.
- [11] H. Khalid, S. Pollin, M. Rykunov, A. Bourdoux and H. Sahli, "Convolutional Long Short-Term Memory Networks for Doppler-Radar based Target Classification," in *Proceedings of the 2019 IEEE Radar Conference, Boston, MA, USA*, pp. 22–26, 2019.
- [12] J. Akhtar and K. E. Olsen, "Go-cfar trained neural network target detectors," in *2019 IEEE Radar Conference (RadarConf)*, Boston, MA, USA, pp. 1–5, 2019.
- [13] C. E. Thornton, M. A. Kozy, R. M. Buehrer, A. F. Martone and K. D. Sherbondy, "Deep reinforcement learning control for radar detection and tracking in congested spectral environments," *IEEE Trans. Cognit. Commun. Netw.*, vol. 6, no. 4, pp. 1335–1349, 2020.
- [14] X. X. Zhu, D. Tuia, L. Mou, G.-S. Xia, L. Zhang, F. Xu and F. Fraundorfer, "Deep learning in remote sensing: A comprehensive review and list of resources," *IEEE Geosci. Remote Sens. Mag.*, vol. 5, no. 4, pp. 8–36, 2017.
- [15] L. Zhang, L. Zhang and B. Du, "Deep learning for remote sensing data: A technical tutorial on the state of the art," *IEEE Geosci. Remote Sens. Mag.*, vol. 4, no. 2, pp. 22–40, 2016.
- [16] L. Wang, J. Tang and Q. Liao, "A Study on Radar Target Detection Based on Deep Neural Networks," in *IEEE Sensors Letters*, vol. 3, no. 3, pp. 1–4, 2019.
- [17] H. Deng, Z. Geng and B. Himed, "Radar Target Detection Using Target Features and Artificial Intelligence," *2018 Int. Conf. on Radar (RADAR), Brisbane, QLD*, pp. 1–4, 2018.
- [18] F. Yavuz and M. Kalfa, "Radar Target Detection via Deep Learning," *2020 28th IEEE Conf. on Signal Processing and Communications Applications (SIU), Gaziantep, Turkey*, pp. 1–4, 2020.
- [19] J. Akhtar and K. Olsen "A Neural Network Target Detector with Partial CA-CFAR Supervised Training," *International Conference on Radar (RADAR), Brisbane, QLD, Australia*, pp. 1–6, 2018.
- [20] M. Mostafa, S. Zahran, A. Moussa, N. El-Sheimy and A. Sesay, "Radar and visual odometry integrated system aided navigation for UAVS in GNSS denied environment," *Sensors*, vol. 18(9), no. 2776, 2018.
- [21] S. Zahran, M. Mostafa, A. Moussa and N. El-Sheimy, "Augmented Radar Odometry by Nested Optimal Filter Aided Navigation for UAVS in GNSS Denied Environment," in *2021 International Telecommunications Conference, ITC-Egypt, Alexandria, Egypt*, pp. 1–5, 2021.
- [22] K. L. Yuan, "Wavelet denoising based on threshold optimization method," *Engineering Journal of Wuhan University*, vol. 48, no. 1, pp. 74–80, 2015.
- [23] H. Masood, A. Zafar, M. U. Ali, M. A. Khan, S. Ahmed et al., "Recognition and tracking of objects in a clustered remote scene environment," *Computers, Materials & Continua*, vol. 70, no. 1, pp. 1699–1719, 2022.
- [24] E. Katz and Y. Barnes, "Comparison of SNR and Peak-SNR (PSNR) as performance measures and signals for peak-limited two-dimensional (2D) pixelated optical wireless communication," in: *Conference on Signals, Systems & Computers. IEEE, Pacific Grove, CA, USA*, pp. 1880–1884, 2015.
- [25] E. B. Quist, P. C. Niedfeldt and R. W. Beard, "Radar odometry with recursive-RANSAC," *IEEE Transactions on Aerospace and Electronic Systems*, vol. 52, no. 4, pp. 1618–1630, 2016